Mathematics

https://www.aimspress.com/journal/Math

AIMS Mathematics, 10(3): 7489–7508.
DOI: 10.3934/math.2025344
Received: 17 January 2025
Revised: 15 March 2025
Accepted: 26 March 2025
Published: 31 March 2025

Research article

Influence of the β-fractional derivative on optical soliton solutions of the pure-quartic nonlinear Schrödinger equation with weak nonlocality

Mahmoud Soliman[1], **Hamdy M. Ahmed**[2], **Niveen Badra**[1], **M. Elsaid Ramadan**[3,*], **Islam Samir**[1] **and Soliman Alkhatib**[4]

[1] Department of Physics and Mathematics Engineering, Faculty of Engineering, Ain Shams University, Cairo, Egypt

[2] Department of Physics and Engineering Mathematics, Higher Institute of Engineering, El Shorouk Academy, Cairo, Egypt

[3] Department of Mathematics, Faculty of Science, Islamic University of Madinah, Medina, Saudi Arabia

[4] College of Engineering and Technology, American University in the Emirates (AUE), Dubai intel Academic City, P. O. Box 503000, Dubai, UAE

* **Correspondence:** Email: m.elsaid@iu.edu.sa.

Abstract: This study investigated the dynamics of a pure-quartic nonlinear Schrödinger equation incorporating a β-fractional derivative and weak nonlocal effects prevalent in optical fiber systems. Using the improved modified extended tanh-function method, we obtained a diverse array of soliton solutions, including bright, dark, and singular solitons, as well as hyperbolic, trigonometric, and Jacobi elliptic solutions. The main goal was to clarify how fractional derivatives, defined by the parameter β, affect the characteristics and behavior of these soliton solutions. The key outcomes indicate that variations in the parameter β lead to substantial changes in soliton amplitude, shape, and propagation patterns. Graphical illustrations clearly depict these transformations, highlighting how fractional derivatives have a major impact on the properties of solitons. Crucially, for certain fractional orders, the localization and stability of solitons are enhanced, which is essential for accurate modeling of nonlocal and dispersive effects in optical fibers. This work not only enhances fundamental understanding of nonlinear wave phenomena within optical communication systems but also offers valuable insights into using fractional calculus for designing and optimizing advanced photonic devices.

Keywords: nonlinear Schrödinger equation; soliton solutions; fractional derivatives; improved modified extended tanh-function method
Mathematics Subject Classification: 35C07, 35C08, 35C09, 35R11

1. Introduction

Because of its potential application in high-speed communication networks, solitons in optical fiber systems have attracted a lot of attention [1–3]. Solitons are special self-sustaining wave packets that do not significantly deform when traveling great distances. They are perfect for dependable information transmission since they maintain their amplitude and shape while propagating [4–6]. Nonlinear wave phenomena have captivated the attention of physicists and mathematicians for centuries, playing a pivotal role in understanding the intricate dynamics of diverse physical systems. From the propagation of light in optical fibers to the behavior of waves in plasmas and condensed matter, nonlinear wave equations have emerged as fundamental tools for describing these complex phenomena. There are many fields that seek soliton solutions, such as plasma physics, which examines the Zakharov equation in weakly nonlinear ion-acoustic phenomena [7], and nonlinear optics [8–10]. Among these equations, the nonlinear Schrödinger equation (NLS) stands out as a cornerstone in the study of nonlinear wave dynamics, finding applications in diverse fields such as optics, fluid mechanics [11, 12], and Bose–Einstein condensates.

The pure-quartic NLS has garnered significant attention in recent years due to its ability to model a variety of physical phenomena, particularly in the context of nonlinear wave dynamics [13–15], specially for Schrodinger equations [16–18], and many papers tried to provide numerical methods to solve such as [19–21]. Unlike traditional cubic NLS equations, which describe standard soliton behavior, the pure-quartic NLS introduces a higher-order nonlinearity that can lead to richer dynamics and more complex wave structures. This nonlinearity allows for the modeling of phenomena such as wave collapse and the formation of localized structures in various media, including optical fibers and Bose-Einstein condensates. Incorporating nonlocal effects into the pure-quartic NLS is essential for accurately describing systems where interactions extend beyond immediate spatial or temporal neighborhoods. Nonlocality is particularly relevant in optical systems, where the propagation of light can be influenced by the nonlocal response of the medium, leading to phenomena that are not captured by local models.

Nonlinear dynamical systems exhibit a wide range of behaviors, including bifurcations, chaotic dynamics, and soliton formation, which are essential in fields such as optics, fluid dynamics, and economic models. Bifurcation theory plays a crucial role in understanding stability transitions and complex system behavior. For instance, previous studies such as [22] have analyzed the bifurcation dynamics of the Kopel triopoly model, highlighting the effects of parameter variations on stability. Similarly, the discrete-time Lotka–Volterra model [23] has been studied using nonstandard finite difference discretization methods to explore its dynamical properties and bifurcations, providing valuable insights into the role of discretization in nonlinear systems.

Additionally, ensemble classifier design methods, such as those based on the perturbation binary salp swarm algorithm [24], have been developed to handle complex classification problems by leveraging perturbation-based optimization techniques. Inspired by these advancements, our study investigates the impact of fractional dispersion and weak nonlocality on soliton formation, exploring how nonlinear interactions influence soliton stability and bifurcation structures within a fractional NLS framework. Understanding these effects contributes to the broader discussion of nonlinear wave phenomena and their stability under varying system parameters. The original model as mentioned in [25, 26] is:

$$iq_t + \frac{1}{24}C_1 q_{xxxx} + C_2|q|^2 q + C_3 q(|q|^2)_{xx} = 0. \tag{1.1}$$

The transition from the classical pure-quartic NLS to its fractional counterpart is motivated by the need to accurately model nonlocal and memory effects in optical wave propagation. In many optical systems, such as highly dispersive fiber optics and photonic crystals, wave dynamics exhibit anomalous dispersion and long-range interactions that cannot be fully captured using integer-order derivatives. The incorporation of a fractional derivative into the pure-quartic NLS serves to generalize the standard model by introducing a history-dependent influence on soliton behavior, so we modify the equation to be:

$$iD_t^{\beta} q + \frac{1}{24}C_1 D_{xxxx}^{\beta} q + C_2|q|^2 q + C_3 q D_{xx}^{\beta}|q|^2 = 0. \tag{1.2}$$

The model in the context of the β-fractional derivative, a generalization of the classical derivative, is discussed in this article. The model equation describes the wave profile of the electric field in an optical fiber, which is represented by the complex-valued function

$$q = q(x, t).$$

The model incorporates several key elements, including the β-fractional derivative D_t^{β}, which governs memory effects and nonlocal dispersion in the system. The coefficients C_1–C_3 represent the strength of fourth-order dispersion, Kerr nonlinearity, and nonlocal interactions, respectively. The model also accounts for spatially extended (weak nonlocal) interactions through the term $D_{xx}^{\beta} q$. The present study focuses on the pure-quartic NLS with weak nonlocality and fractional dispersion, which effectively captures the influence of fourth-order dispersion on soliton dynamics. However, it does not explicitly account for higher-order dispersion terms such as fifth-order dispersion or additional nonlinear interactions like self-steepening or Raman scattering effects. The authors suggest that future work could extend the current model by incorporating these higher-order effects, leading to a more general fractional NLS. This could be achieved through numerical simulations and analytical techniques, which could provide insights into the stability, collision dynamics, and spectral properties of soliton solutions in highly nonlinear optical systems [27–29].

The study explores the concept of fractional derivatives, which offer a powerful framework for capturing nonlocal effects in real-world systems. Fractional calculus has numerous applications, including modeling wave propagation through incompressible fluids and shallow water [30], the behavior of molecules and materials [31, 32], and applications in circuit theory and biology [33].

The generalized β fractional derivative nonlinear Schrödinger (GBFNS) equation presents a generalized framework where soliton properties can be continuously tuned via the fractional derivative parameter β. This feature allows for a deeper exploration of the transition between classical solitons and rogue-like structures under varying degrees of nonlocality and dispersion. Furthermore, symbolic computation methods, similar to those used in the derivation of lump solutions, such as the (3+1)-dimensional Hirota–Satsuma–Ito equation [34], and lump solutions in spatially symmetric generalized Kadomtsev–Petviashvili models [35], could be extended to fractional wave equations to identify novel solution families. Moreover, Darboux transformations have been widely employed to generate N-soliton solutions in integrable systems, including modified Korteweg–de–Vries-type equations [36, 37]. Incorporating Darboux-based approaches into the fractional-order framework may enable the construction of multi-soliton and breather solutions within the GBFNS equation. Future work could explore how these methods can be adapted to study the interaction dynamics of fractional solitons, including the potential emergence of rogue wave-type structures in nonlocal optical systems. The key contributions of this work are now clearly stated, emphasizing the combination of fractional derivatives, weak nonlocality, and the improved modified extended tanh-function method (IMETM) to obtain soliton solutions. Unlike previous studies, our approach considers higher-order dispersion effects in fractional systems, leading to new insights into soliton dynamics. Additionally, we discuss how fractional-order dispersion modifies soliton behavior, providing a broader understanding of nonlinear wave propagation in optical and complex media.

The paper is structured as follows: Section 2 provides preliminary definitions and properties of the fractional beta derivative. Section 3 presents the IMETM as a powerful technique for solving nonlinear fractional differential equations. Section 4 demonstrates the application of the IMETM to the GBFNS equation, leading to the derivation of novel solitary wave solutions. Section 5 provides a graphical illustration of some obtained solutions showing the characteristics of solutions under different fractional orders. Section 6 discusses the obtained results with previous literature. Finally, Section 7 concludes the paper, summarizing the main findings.

2. Preliminaries

Definition 1. [38] Let f be a function such that

$$f : [a, \infty) \to \mathbb{R}.$$

Then, the beta derivative of a function f is defined as

$$D_t^{\beta} f(t) = \lim_{\epsilon \to 0} \frac{f\left(t + \epsilon\left(t + \frac{1}{\Gamma(\beta)}\right)^{1-\beta}\right) - f(t)}{\epsilon},$$

for all $t \geq a, \beta \in (0, 1]$. Then, if the limit of the above exists, f is said to be β-differentiable.

The fractional derivative D^{β} used in this study satisfies several important properties, which we summarize below:

$$D^{\beta}\left(af(t) + bg(t)\right) = aD^{\beta} f(t) + bD^{\beta} g(t), \quad \forall a, b \in \mathbb{R}, \quad \text{(linearity)},$$

$$D^{\beta}\left(f(t)g(t)\right) = f(t)D^{\beta} g(t) + g(t)D^{\beta} f(t), \quad \text{(product rule)},$$

$$D^{\beta}\left(\frac{f(t)}{g(t)}\right) = \frac{g(t)D^{\beta} f(t) - f(t)D^{\beta} g(t)}{(g(t))^2}, \quad \text{(quotient rule)},$$

$$D^{\beta} f(t) = (t + \frac{1}{\Gamma(\beta)})^{1-\beta} \frac{df(t)}{dt}, \quad \text{(fundamental definition)},$$

$$D^{\beta}\left(f(g(t))\right) = g'(t)^{\beta} D^{\beta} f(g(t)), \quad \text{(fractional chain rule)}.$$

3. The referenced methodology: IMETM

In the works [39–41], the IMETM methodology is thoroughly articulated. Consider the non-linear partial differential equation (NLPDE) shared below:

$$\mathcal{Y}(U, D_t^{\beta} U, D_x^{\beta} U, D_{xx}^{\beta} U, D_{tt}^{\beta} U, ...) = 0. \tag{3.1}$$

Implementing the approach advanced in this study necessitates traversing through enumerated procedures:

Step 1: To begin, use the wave transformation explained below to convert the NLPDE in Eq (3.1) to its corresponding ordinary differential equation (ODE):

$$U(x,t) = u(z)e^{i\phi}, \quad z = \frac{h\left(\frac{1}{\Gamma(\beta)} + x\right)^{\beta}}{\beta}, \quad \phi = \theta + \frac{\omega\left(\frac{1}{\Gamma(\beta)} + t\right)^{\beta}}{\beta}.$$

The wave propagation direction is represented by h, the order of fractional derivative is denoted as β, wave number is indicated by ω, and the phase constant can be referred to as θ. Subsequently, Eq (3.1) transforms into:

$$\mathcal{R}(u, u', u'', u^{(3)}, u^{(4)}, ...) = 0. \tag{3.2}$$

Step 2: Represent the ODE solution with the formula:

$$u(z) = s_0 + \sum_{j=1}^{N} s_{2j} \frac{1}{\lambda^j(z)} + \sum_{j=1}^{N} s_{2j-1} \lambda^j(z), \tag{3.3}$$

where s_{2j} and $s_{2j-1} \neq 0$, and at same time, $\lambda(z)$ fulfills the differential equation:

$$\lambda'(z) = \sqrt{p_0 + p_1\lambda(z) + p_2\lambda^2(z) + p_3\lambda^3(z) + p_4\lambda^4(z)}. \tag{3.4}$$

Step 3: The choice of N in Eq (3.3) hinges on the balance method, derived from analysis on Eq (3.2).

3.1. Balance principle for determining N

To ensure a consistent solution structure, we apply the balance principle, which determines the highest power N in the assumed series solution. This principle equates the dominant terms in the highest-order derivative and the nonlinear terms. The balance principle requires comparing:

(1) The highest-order derivative term in the governing equation.

(2) The highest-order nonlinear term in the equation.

Let m be the highest order of differentiation appearing in the equation; p be the highest exponent of q in the nonlinear terms; k be an integer shift factor that depends on the structure of the nonlinear term (e.g., if a nonlinear term involves a derivative of q, k accounts for that differentiation). From the governing equation, the highest-order derivative term contributes a leading order of $N - m$, while the highest nonlinear term contributes an order of $pN + k$. Setting these powers equal gives the balance condition:

$$N - m = pN + k.$$

Solving for N, we obtain

$$N = \frac{m-k}{1-p}.$$

For a valid solution, N must be a non-negative integer, which imposes constraints on the system parameters. Applying the balance condition ensures the validity of the solution ansatz and helps determine the appropriate power series expansion.

Step 4: Create a set of nonlinear algebraic equations by inserting the proposed solutions into Eq (3.3) and utilizing Eq (3.4) to substitute in Eq (3.2). Afterwards, ensure that each coefficient of $\lambda^h(z)$ for $h = 0, 1, 2, \ldots$ equals zero through equating.

Step 5: Use software like Mathematica to solve the algebraic system, determining the coefficients s_{2j}, s_{2j-1}, ω, and k.

Step 6: Distinct numerical values for p_0–p_4 yield different types of solutions:

Case 1. With $p_0 = p_1 = p_3 = 0$,

$$\lambda(z) = \sqrt{-\frac{p_2}{p_4}}\operatorname{sech}(\sqrt{p_2}z), \quad p_2 > 0, \quad p_4 < 0,$$

$$\lambda(z) = \sqrt{-\frac{p_2}{p_4}}\sec(\sqrt{-p_2}z), \quad p_2 < 0, \quad p_4 > 0.$$

Case 2. For $p_1 = p_3 = 0$, $p_0 = \frac{p_2^2}{4p_4}$,

$$\lambda(z) = \sqrt{\frac{-p_2}{2p_4}}\tanh(\sqrt{\frac{-p_2}{2}}z), \quad p_2 < 0, \quad p_4 > 0,$$

$$\lambda(z) = \sqrt{\frac{p_2}{2p_4}}\tan(\sqrt{\frac{p_2}{2}}z), \quad p_2 > 0, \quad p_4 > 0.$$

Case 3. For $p_4 = p_3 = 0$,

$$\lambda(z) = \frac{-p_1}{2p_2}\sinh(2\sqrt{p_2}z) - \frac{p_1}{2p_2}, \quad p_2 > 0, \quad p_0 = 0,$$

$$\lambda(z) = e^{\sqrt{p_2}z} - \frac{p_1}{2p_2}, \quad p_2 > 0, \quad p_0 = \frac{p_1^2}{4p_2}.$$

Case 4. When $p_0 = p_1 = 0$,

$$\lambda(z) = \frac{-p_2}{p_3}(\tanh(\frac{\sqrt{p_2}}{2}z) + 1), \quad p_2 > 0, \quad p_4 = \frac{p_3^2}{4p_2}.$$

Case 5. For the condition $p_1 = p_3 = 0$,

$$\lambda(z) = \sqrt{\frac{-p_2m^2}{p_4(2m^2-1)}}\operatorname{cn}(\sqrt{\frac{p_2}{(2m^2-1)}}z), \quad p_2 > 0, \ \ p_4 < 0, \ \ p_0 = \frac{p_2^2m^2(1-m^2)}{p_4(2m^2-1)^2},$$

$$\lambda(z) = \sqrt{-\frac{m^2}{p_4(2-m^2)}}\operatorname{dn}(\sqrt{\frac{p_2}{(2-m^2)}}z), \quad p_2 > 0, \ \ p_4 < 0, \ \ p_0 = \frac{p_2^2(1-m^2)}{p_4(2-m^2)^2},$$

$$\lambda(z)=\sqrt{-\frac{p_2m^2}{p_4(1+m^2)}}\mathrm{sn}(\sqrt{\frac{-p_2}{(1+m^2)}}z),\quad p_2<0,\ \ p_4>0,\ \ p_0=\frac{p_2^2m^2}{p_4(1+m^2)^2}.$$

The Table 1 provides clarity on how the Jacobi elliptic functions behave as the parameter m approaches 0 or 1. As seen some of them oscillate between trigonometric functions and hyperbolic ones.

Table 1. Behavior of Jacobi elliptic functions as m approaches 0 and 1.

Function	Limit as $m\to 0$	Limit as $m\to 1$
$\mathrm{sn}(u,m)$	$\mathrm{sn}(u,0)=\sin(u)$	$\mathrm{sn}(u,1)=\tanh(u)$
$\mathrm{cn}(u,m)$	$\mathrm{cn}(u,0)=\cos(u)$	$\mathrm{cn}(u,1)=0$
$\mathrm{dn}(u,m)$	$\mathrm{dn}(u,0)=1$	$\mathrm{dn}(u,1)=\mathrm{sech}(u)$
$\mathrm{sc}(u,m)$	$\mathrm{sc}(u,0)=1$	$\mathrm{sc}(u,1)=\infty$
$\mathrm{cs}(u,m)$	$\mathrm{cs}(u,0)=1$	$\mathrm{cs}(u,1)=0$
$\mathrm{ns}(u,m)$	$\mathrm{ns}(u,0)=1$	$\mathrm{ns}(u,1)=1$
$\mathrm{nc}(u,m)$	$\mathrm{nc}(u,0)=1$	$\mathrm{nc}(u,1)=0$

These transformations provide a clearer interpretation of the solutions in the context of both periodic and hyperbolic behaviors, enhancing the understanding of the dynamics captured by the β-fractional derivative NLS.

Step 7. Integrating the multiple coefficients s_j and s_{j+1} with the solutions obtained, numerous solutions to Eq (3.1) are extracted.

The IMETM has proven to be a valuable tool for deriving soliton solutions for partial differential equations. One of the key strengths of the IMETM is its ability to find a wide range of soliton solutions, including bright, dark, and singular solitons, as well as periodic solutions and trigonometric solutions. This is compared to many other methods such as Kudryashov method, sine-Gordon expansion, or variational approaches that may struggle to obtain such a diverse set of solutions. However, it is also important to acknowledge the limitations of the IMETM. When the balance parameter N is large, the method can become increasingly complex and difficult to apply. This is because the number of terms in the solution expansion grows rapidly with N, making it challenging to obtain a tractable solution. In such cases, other methods may be more suitable, and a combination of approaches may be necessary to fully understand the behavior of the system.

4. Applications of the studied model

We seek to obtain exact soliton solutions for Eq (1.2) through the following approach:

$$q(x,t)=Q(z)e^{i\phi},\quad z=\frac{h\left(\frac{1}{\Gamma(\beta)}+x\right)^{\beta}}{\beta},\quad \text{and}\quad \phi=\theta+\frac{\omega\left(\frac{1}{\Gamma(\beta)}+t\right)^{\beta}}{\beta}. \tag{4.1}$$

The phase term ϕ primarily accounts for wave oscillations and soliton velocity. However, in fractional systems, this phase function plays a more complex role. The fractional exponent in ϕ modifies the dispersion relation, making the soliton velocity explicitly dependent on the fractional order β. This modification introduces anomalous dispersion effects, enabling solitons to propagate at non-integer power scaling rates rather than the linear propagation observed in classical systems. Unlike standard solitons, which obey a fixed dispersion-speed relationship, fractional solitons exhibit memory-dependent velocity adjustments, leading to variable soliton width and amplitude. As a result, the phase term ensures that the soliton profile dynamically adapts to fractional-order dispersion, allowing for enhanced stability under varying nonlocal and dispersive conditions. The parameter h is a scaling factor that influences the soliton amplitude and width, playing a crucial role in shaping the soliton's spatial structure. The frequency parameter ω determines the propagation speed and oscillation rate of the soliton, directly affecting its phase evolution. The constant θ represents the initial phase shift, which influences the soliton's initial position and interaction with the surrounding medium. These parameters collectively govern the soliton's behavior in a fractional system, ensuring adaptability under different dispersion and nonlocality conditions.

By inserting Eq (4.1) into Eq (1.2), we are able to transform the fractional NLPDE into a ODE, resulting in the following outcome:

$$C_1h^4Q^{(4)}(z) + 48C_3h^2Q(z)^2Q''(z) - 24Q(z)\left(\omega - 2C_3h^2Q'(z)^2\right) + 24C_2Q(z)^3 = 0. \tag{4.2}$$

To carry out the suggested technique, it is essential to compute an integer value for N. The calculation of this value involves balancing $Q^{(4)}$ with $Q(z)^2Q''(z)$ in Eq (4.2) and determining that

$$N = 1.$$

Afterwards, we can express the solution to the resulting ordinary differential equation as follows:

$$Q(z) = s_0 + s_1\lambda(z) + \frac{s_2}{\lambda(z)}. \tag{4.3}$$

Equations (4.3) and (3.4) are substituted into Eq (4.2) to solve Eq (1.2). The system of nonlinear algebraic equations that emerges from equating the coefficients of $\lambda(z)$ to zero is handled by Mathematica software packages. To obtain exact soliton solutions, we employed Mathematica to solve the resulting algebraic systems derived from the IMETM. The computational process involved symbolic manipulation, equation simplification, and the use of polynomial system solvers to determine the unknown parameters. The complexity of solving these algebraic systems depends on the number of unknown parameters and the degree of the nonlinear terms. In our case, the symbolic computation required solving polynomial equations of a degree of 6, with multiple coupled nonlinear constraints. The worst-case computational complexity for polynomial equation solving is exponential in the number of variables, but Mathematica optimizes this process using Gröbner bases and elimination techniques. On a standard machine (Intel Core i5-7200u, 8GB RAM), the execution time for solving the algebraic system varied between 1 and 5 minutes, depending on the specific parameter choices and system constraints. Larger solution spaces and higher-order polynomial terms required more computation time due to increased symbolic simplifications.

This yields the following outcomes for Eq (1.2):

Case 1. $p_0 = p_1 = p_3 = 0$,

$$s_0 = 0, \quad s_2 = 0, \quad \omega = -\frac{C_3h^2p_2^2s_1^2}{4p_4}, \quad p_4 = -\frac{6C_3s_1^2}{C_1h^2}, \quad p_2 = \frac{C_2}{C_3h^2}.$$

For Eq (1.2), we are able to provide both a singular solution and a bright soliton solution:

$$q_1(x,t) = \sqrt{\frac{C_1C_2}{6C_3^2}}\,\mathrm{sech}\left(\frac{1}{\beta}\sqrt{\frac{C_2}{C_3}}\left(\frac{1}{\Gamma(\beta)}+x\right)^{\beta}\right)e^{\mathrm{i}\phi}, \quad \text{for } C_1C_2>0,\ C_2C_3>0, \tag{4.4}$$

$$q_2(x,t) = \sqrt{\frac{C_1C_2}{6C_3^2}}\,\sec\left(\frac{1}{\beta}\sqrt{\frac{-C_2}{C_3}}\left(\frac{1}{\Gamma(\beta)}+x\right)^{\beta}\right)e^{\mathrm{i}\phi}, \quad \text{for } C_1C_2>0,\ C_2C_3<0. \tag{4.5}$$

Case 2. $p_1 = p_3 = 0, p_0 = \frac{p_2^2}{4p_4}$,

$$s_0 = 0, \quad s_1 = \frac{2p_4s_2}{p_2}, \quad \omega = -4C_3h^2p_4s_2^2, \quad p_2 = -\frac{C_2}{2C_3h^2}, \quad p_4 = -\frac{C_1h^2p_2^2}{24C_3s_2^2}.$$

Following this, singular soliton and singular periodic solutions can be offered for Eq (1.2):

$$q_3(x,t) = \sqrt{\frac{-C_1C_2}{6C_3^2}}\,\mathrm{csch}\left(\frac{1}{\beta}\sqrt{\frac{C_2}{C_3}}\left(\frac{1}{\Gamma(\beta)}+x\right)^{\beta}\right)e^{\mathrm{i}\phi}, \tag{4.6}$$

for $C_2C_3>0,\ C_1C_2<0$,

$$q_4(x,t) = \sqrt{\frac{C_1C_2}{6C_3^2}}\,\csc\left(\frac{1}{\beta}\sqrt{\frac{C_2}{C_3}}\left(\frac{1}{\Gamma(\beta)}+x\right)^{\beta}\right)e^{\mathrm{i}\phi}, \tag{4.7}$$

for $C_2C_3<0,\ C_1C_2>0$.

Case 3. $p_3 = p_4 = 0$. For $p_0 = 0$, we get this set of solutions:

$$s_0 = \frac{p_1s_1}{2p_2}, \quad s_2 = 0, \quad \omega = \frac{C_1h^4p_2^3 - 12C_3h^2p_1^2s_1^2}{24p_2}, \quad C_2 = -4C_3h^2p_2,$$

and for

$$p_0 = \frac{p_1^2}{4p_2},$$

we get this set of solutions:

$$s_0 = \frac{p_2s_2}{p_1}, \quad s_1 = 0, \quad \omega = -\frac{C_3h^2p_2^3s_2^2}{2p_1^2}, \quad C_1 = -\frac{24C_3p_2s_2^2}{h^2p_1^2}, \quad C_2 = -\frac{1}{2}C_3h^2p_2.$$

Subsequently, hyperbolic and exponential solutions can be presented for Eq (1.2):

$$q_5(x,t) = \frac{p_1s_1}{2p_2}\sinh\left(\frac{2h\sqrt{p_2}\left(\frac{1}{\Gamma(\beta)}+x\right)^{\beta}}{\beta}\right)e^{\mathrm{i}\phi}, \tag{4.8}$$

for $p_0 = 0, p_2 > 0$,

$$q_6(x,t) = s_2\left(\frac{1}{e^{\frac{h\sqrt{p_2}\left(\frac{1}{\Gamma(\beta)}+x\right)^{\beta}}{\beta}} - \frac{p_1}{2p_2}} + \frac{p_2}{p_1}\right)e^{\mathrm{i}\phi}, \tag{4.9}$$

for

$$p_2 > 0, \quad p_0 = \frac{p_1^2}{4p_2}.$$

Case 4. $p_0 = p_1 = 0$,

$$s_0 = \frac{\sqrt{p_2 p_4} s_1}{2p_4}, \quad s_2 = 0, \quad \omega = -\frac{C_3 h^2 p_2^2 s_1^2}{8p_4}, \quad p_4 = -\frac{6C_3 s_1^2}{C_1 h^2}, \quad p_2 = -\frac{2C_2}{C_3 h^2}.$$

Following this, a dark soliton solution is demonstrated in Eq (1.2),

$$q_7(x,t) \;\; = \frac{\sqrt{C_1 C_2}}{2C_3\sqrt{3}} \tanh\left(\frac{1}{\beta}\sqrt{-\frac{C_2}{2C_3}}\left(\frac{1}{\Gamma(\beta)} + x\right)^{\beta}\right) e^{\mathrm{i}\phi}, \tag{4.10}$$

for

$$p_3^2 = 4p_2 p_4, \quad C_2 C_3 < 0, \quad C_1 C_2 > 0.$$

Case 5. $p_3 = p_1 = 0$,

$$s_0 = 0, \quad s_2 = 0, \quad \omega = -\frac{C_3 h^2 \left(p_2^2 + 4p_0 p_4\right) s_1^2}{4p_4}, \quad C_1 = -\frac{6C_3 s_1^2}{h^2 p_4}, \quad C_2 = C_3 h^2 p_2.$$

After that, Eq (1.2) can have Jacobi elliptic solutions as shown:

$$q_8(x,t) = \sqrt{\frac{C_1 C_2 m^2}{6C_3^2 (2m^2 - 1)}} \mathrm{cn}\left(\frac{\left(x + \frac{1}{\Gamma(\beta)}\right)^{\beta} \sqrt{\frac{C_2}{C_3}}}{\beta}, m\right) e^{\mathrm{i}\phi}, \tag{4.11}$$

for

$$\frac{C_1 C_2}{2m^2 - 1} > 0, \quad \frac{C_2}{C_3} > 0, \quad 0 < m < 1;$$

$$q_9(x,t) = \sqrt{\frac{C_1 m^2}{6C_3 (2 - m^2)}} \mathrm{dn}\left(\frac{\left(x + \frac{1}{\Gamma(\beta)}\right)^{\beta} \sqrt{\frac{C_2}{(2-m^2)C_3}}}{\beta}, m\right) e^{\mathrm{i}\phi}, \tag{4.12}$$

for

$$\frac{C_1}{C_3} > 0, \quad \frac{C_2}{C_3} > 0, \quad 0 < m < 1;$$

$$q_{10}(x,t) = \sqrt{\frac{C_1 C_2 m^2}{6C_3^2 (m^2 + 1)}} \mathrm{sn}\left(\frac{\left(x + \frac{1}{\Gamma(\beta)}\right)^{\beta} \sqrt{-\frac{C_2}{(m^2+1)C_3}}}{\beta}, m\right) e^{\mathrm{i}\phi}, \tag{4.13}$$

for

$$C_1 C_2 > 0, \quad \frac{C_2}{C_3} < 0, \quad 0 < m < 1.$$

5. Graphical visualization of solutions

Graphical representations are utilized to showcase the features of the obtained results for selected solutions. In Figure 1, was simulate the bright optical soliton solution described by Eq (4.4) with different values of β, using

$$C_1 = 1.65, \quad C_2 = 1, \quad C_3 = 2.71.$$

Figure 2 represents contour plots for different values of β to compare between the widths of solitons.

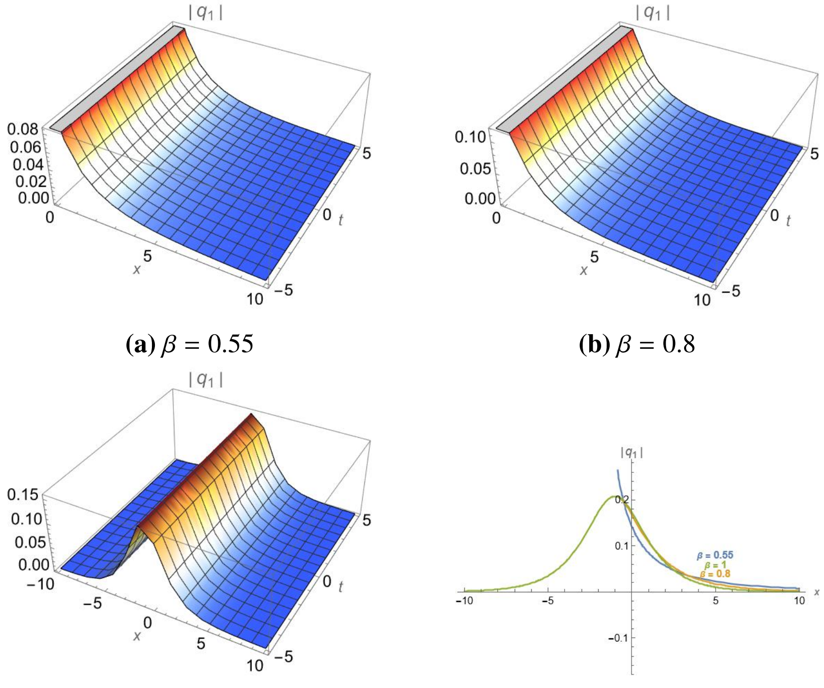

(a) $\beta = 0.55$ **(b)** $\beta = 0.8$

(c) $\beta = 1$ **(d)**

Figure 1. Graphical visualization of hyperbolic solution Eq (4.4).

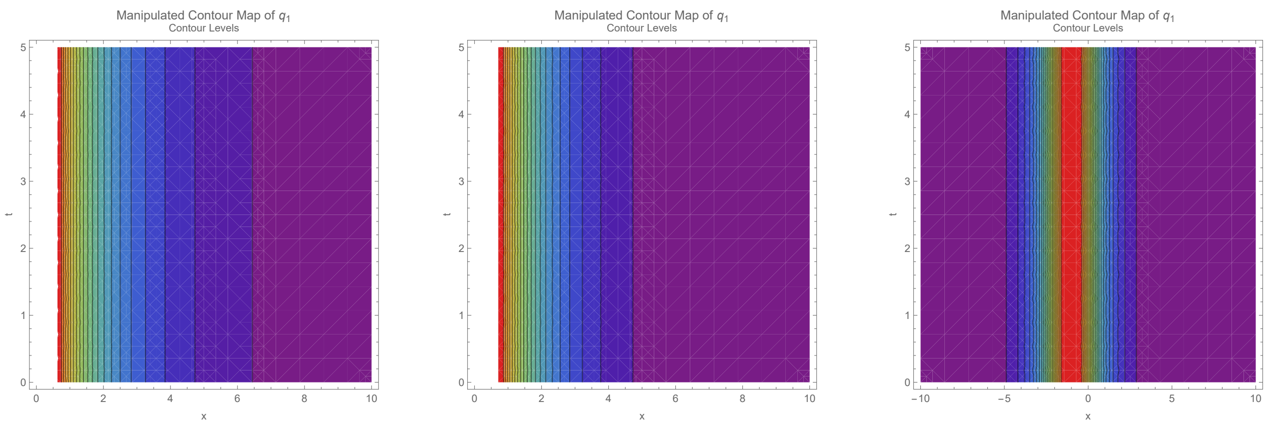

(a) $\beta = 0.55$ **(b)** $\beta = 0.8$ **(c)** $\beta = 1$

Figure 2. Graphical contour plot of hyperbolic solution Eq (4.4).

Similarly, Figure 3 illustrates the dark optical soliton solution of Eq (4.10) with

$$C_1 = 2.48, \quad C_2 = 0.75, \quad C_3 = -1.09,$$

for various β values. Figure 4 represents contour plots for different values of β to compare between the widths of solitons for the dark soliton solution.

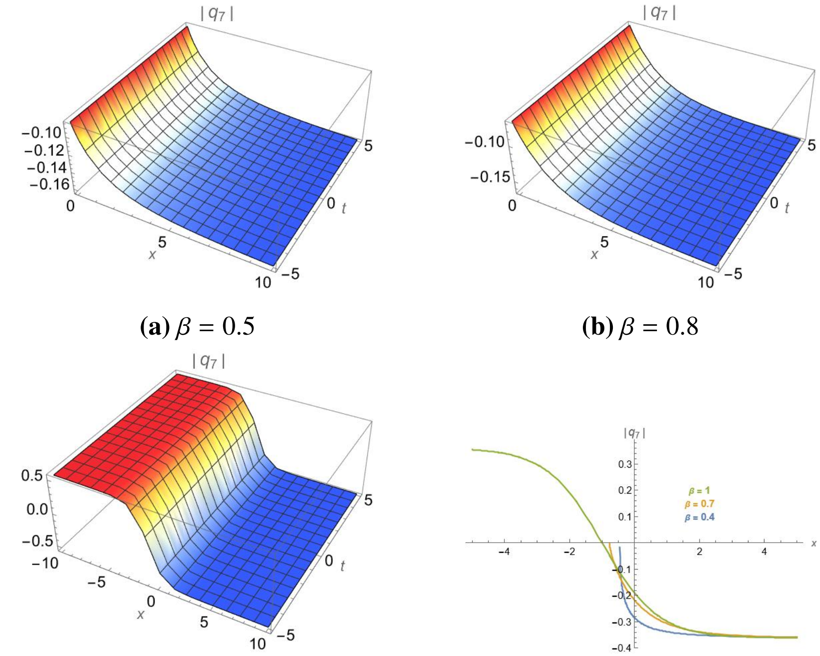

(a) $\beta = 0.5$ **(b)** $\beta = 0.8$

(c) $\beta = 1$ **(d)**

Figure 3. Simulation of another hyperbolic solution Eq (4.10).

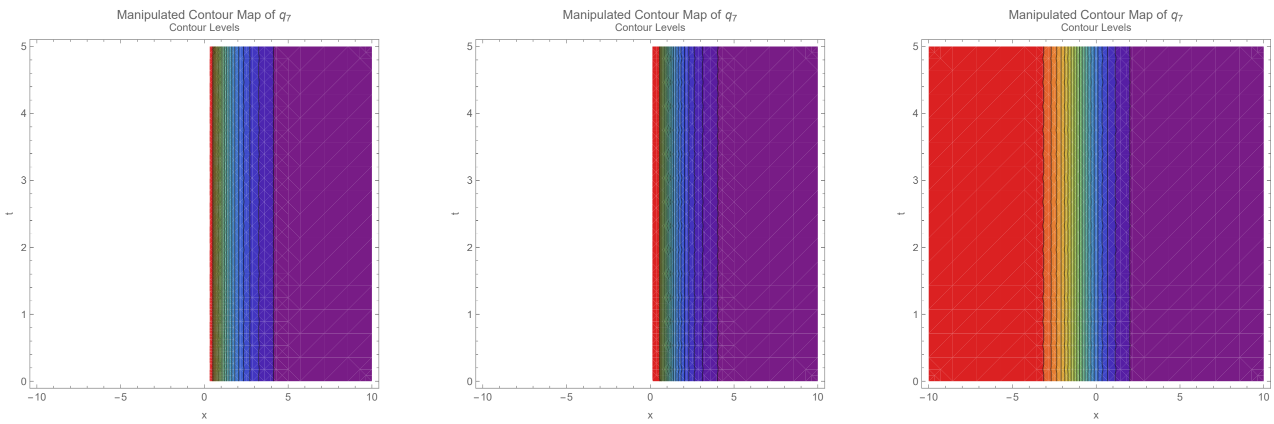

(a) $\beta = 0.5$ **(b)** $\beta = 0.8$ **(c)** $\beta = 1$

Figure 4. Simulation of contour plot solution Eq (4.10).

Additionally, Figure 5 presents a graph of the periodic solution of Eq (4.11) with

$$C_1 = 1.35, \quad C_2 = 1, \quad C_3 = 2.61, \quad \text{and} \quad m = 0.84,$$

demonstrating the effect of different β values. The 2D graphs are drawn at $t = 4$. Figure 6 presents a graph of the singular soliton solution of Eq (4.6) with $C_1 = -1.15$, $C_2 = 1.14$, $C_3 = 1.14$, demonstrating the effect of different β values. The 2D graphs are drawn at $t = 4$.

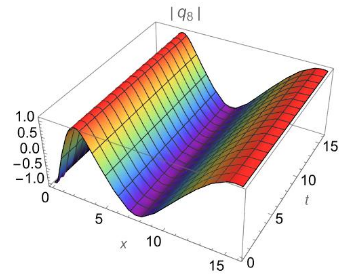

(a) $\beta = 0.55$

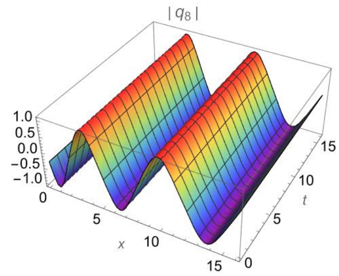

(b) $\beta = 0.8$

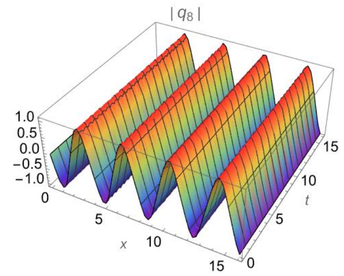

(c) $\beta = 1$

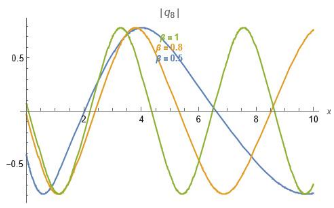

(d)

Figure 5. Visualization of periodic solution Eq (4.11).

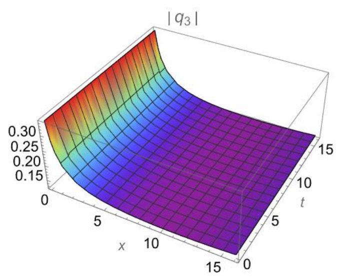

(a) $\beta = 0.55$

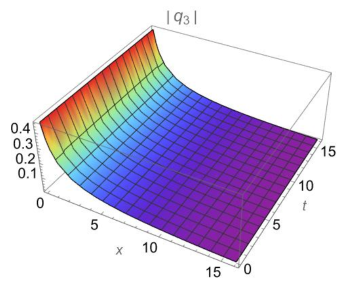

(b) $\beta = 0.8$

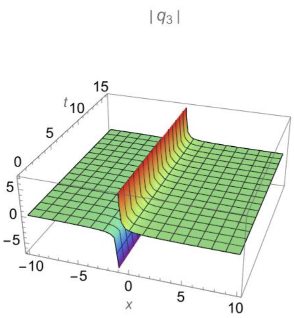

(c) $\beta = 1$

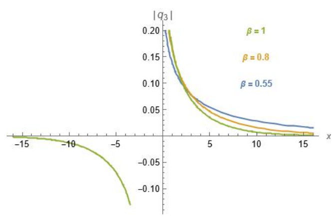

(d)

Figure 6. Visualization of singular soliton solution Eq (4.6).

Figure 7 presents a graph of the trigonometric solution of Eq (4.7) with

$$C_1 = 1.38, \quad C_2 = 1.14, \quad C_3 = 1.5,$$

demonstrating the effect of different β values. The 2D graphs are drawn at $t = 4$.

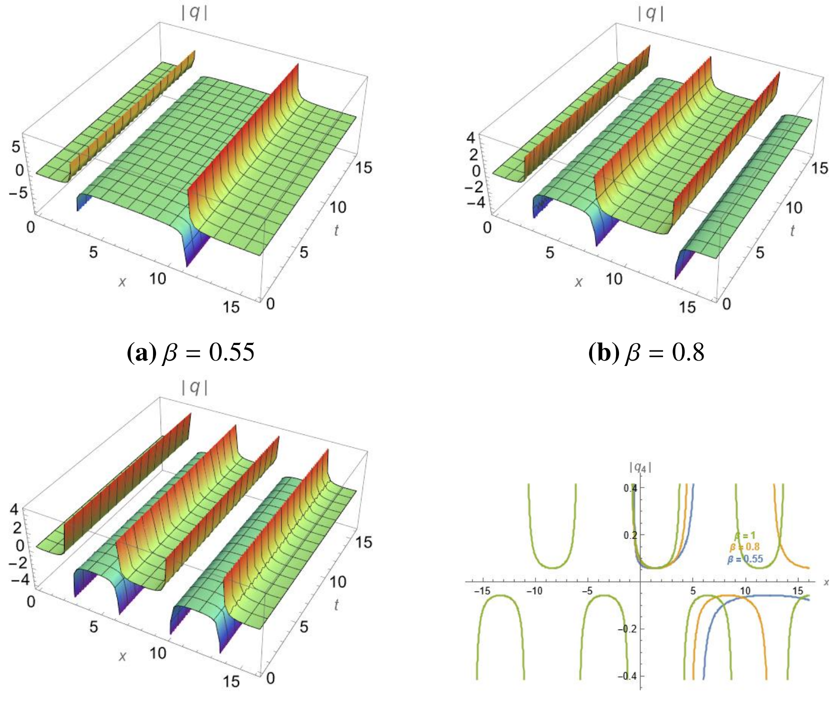

(a) $\beta = 0.55$ **(b)** $\beta = 0.8$

(c) $\beta = 1$ **(d)**

Figure 7. Visualization of trigonometric solution Eq (4.7).

The capability to manipulate and fine-tune soliton properties and make use of the fractional derivative parameter β creates new opportunities for optical communication system design and optimization for photonic devices. The graphical representations show how this parameter affects soliton solutions, highlighting the significance of including fractional calculus in modeling dispersive and nonlocal systems. One of the key findings of this study is that small variations in the fractional order parameter β lead to significant changes in soliton characteristics, including amplitude, width, and propagation speed. This sensitivity poses potential challenges for designing and optimizing optical systems, as minor fluctuations in β could impact soliton stability and interaction dynamics. However, this property also provides a distinct advantage: the ability to fine-tune soliton properties by adjusting β, which is not feasible in classical integer-order models. In optical fiber communication systems, such control could allow for adaptive dispersion management and tunable soliton-based signal transmission. Additionally, fractional-order models enable a broader range of soliton behaviors, making them highly versatile for photonic device applications. To address the potential challenges of sensitivity to β, future research could explore stabilization techniques such as external feedback control, engineered dispersion profiles, or hybrid integer-fractional models that balance flexibility with robustness. Experimental validation of fractional soliton dynamics in structured optical media would also provide insights into practical implementation strategies.

6. Discussion

The importance of using fractional calculus to model dispersive and nonlocal systems lies in their complex dynamics, characterized by non-integer orders. Dispersive systems exhibit frequency-dependent propagation, while nonlocal systems show interactions that extend beyond immediate spatial or temporal neighborhoods.

Previous studies, such as [25,26], explored soliton dynamics in traditional models without fractional derivatives and found that soliton stability could be maintained under certain conditions. However, these models did not capture the nuanced behavior observed in fractional calculus. Our results show that the parameter β significantly influences soliton characteristics, allowing better control over their amplitude and shape.

Graphical representations of soliton solutions obtained through fractional calculus provide insights into these systems, aiding the development of advanced photonic technologies. For instance, at ($\beta = 1$) Eq (4.4) yields a complete bright soliton, while varying β results in distinct wave shapes. Similarly, Eq (4.10) produces a complete dark soliton at ($\beta = 1$) with varying wave forms at other β values. Moreover, Eq (4.11) indicates that while β affects wave propagation, it does not alter wave shape, contrasting with findings in [25, 26], which maintained shape consistency regardless of parameter variations.

The soliton solutions obtained in this study exhibit distinct differences in amplitude, shape, and stability compared to previously known solutions in [25, 26]. One of the key distinctions arises from the inclusion of the β-fractional derivative, which introduces additional flexibility in controlling soliton characteristics. In classical pure-quartic soliton solutions, such as those in [25], soliton profiles remain nearly symmetric with a fixed amplitude and shape determined by the Kerr nonlinearity and fourth-order dispersion. In contrast, our results show that fractional-order dispersion, controlled by β, allows for tunability in both soliton amplitude and width. Specifically, as β decreases from 1, solitons exhibit an increase in peak intensity while becoming more localized, which is a unique feature not observed in integer-order models. Furthermore, compared to [26], which considers weak nonlocal effects in an integer-order framework, our solutions reveal a broader variety of soliton types, including bright, dark, and singular solitons, as well as Jacobi elliptic function solutions. The presence of fractional nonlocality results in more gradual soliton decay and enhanced localization effects. Graphical comparisons indicate that the solitons obtained here exhibit greater robustness against perturbations, suggesting improved stability under weak nonlocal interactions. Additionally, the phase structure of solitons in our model is more dynamically adjustable, allowing for better control over their propagation behavior. Unlike the prior works where soliton characteristics were primarily dictated by the Kerr coefficient and fourth-order dispersion, our results demonstrate that fractional derivatives enable a continuous transformation between different soliton regimes, making the solutions more adaptable to practical optical applications. These findings highlight the potential advantages of fractional-order models in designing and optimizing optical communication systems.

7. Conclusions

The analytical solutions derived in this study provide valuable insights into the dynamics of the GBFNS, particularly in optical fiber systems with weak nonlocal effects. The use of the IMETM has yielded a variety of soliton solutions, including bright, dark, and singular solitons, as well as hyperbolic, trigonometric, and Jacobi elliptic solutions. Notably, the parameter β significantly influences the shape, amplitude, stability, and interaction behaviors of the solitons.

The fractional-order parameter, β, controls the impact on the solitons' characteristics. As β approaches unity, the fractional derivative converges to the classical integer-order derivative, and the solutions resemble those obtained from traditional methods. However, for fractional orders far from unity, the solutions exhibit distinct features, highlighting the nonlocal effects in wave dynamics.

The derived solutions include various soliton types, each with unique characteristics. Bright solitons show a localized peak, dark solitons have a dip in the background intensity, and singular solitons possess an infinite peak at a specific point. The diversity of these solutions underscores the complexity of the GBFNS equation in modeling nonlinear wave phenomena.

Comparing our solutions to those from traditional integer-order derivatives reveals significant differences [25, 26]. Fractional-order derivative solutions demonstrate higher localization, faster propagation, and more complex interactions. This comparison emphasizes the importance of fractional derivatives in modeling real-world systems with substantial nonlocal effects.

The derived solitons in this study have significant real-world implications, particularly in nonlinear optics and fiber optic communications. The bright and dark solitons can be utilized in dispersion-managed fiber systems to maintain signal integrity over long distances, reducing transmission losses and distortion. Additionally, the presence of fractional dispersion makes these solitons highly relevant for mode-locked lasers, where tunable pulse durations are essential for ultrafast optical signal processing. Beyond optics, the findings have applications in plasma physics and Bose–Einstein condensates, where similar nonlinear Schrödinger-type equations govern wave propagation. The inclusion of weak nonlocality and fractional derivatives also introduces unique dispersion properties that could be exploited in metamaterials and engineered optical systems for advanced wave manipulation.

Furthermore, the soliton stability analysis ensures their robustness, making them suitable for optical computing and photonic crystal applications. By addressing these real-world connections, our study bridges the gap between mathematical soliton theory and practical implementation in modern photonics and wave dynamics.

While this method produces diverse solutions, including bright, dark, and singular solitons, large values of N, determined by the balance rule, lead to more complex systems that are challenging to solve.

Author contributions

Mahmoud Soliman: formal analysis, software, writing—original draft; Hamdy M. Ahmed: methodology, validation, writing—review & editing; Niveen Badra: supervision, visualization; M. Elsaid Ramadan: investigation, writing—original draft; Islam Samir: investigation, writing—review & editing; Soliman Alkhatib: conceptualization, writing—review & editing. All authors have read and agreed to the published version of the manuscript.

Use of Generative-AI tools declaration

The authors declare they have not used Artificial Intelligence (AI) tools in the creation of this article.

Conflict of interest

All authors declare no conflicts of interest in this paper.

References

1. P. Li, S. Shi, C. Xu, M. U. Rahman, Bifurcations, chaotic behavior, sensitivity analysis and new optical solitons solutions of Sasa-Satsuma equation, *Nonlinear Dyn.*, **112** (2024), 7405–7415. https://doi.org/10.1007/s11071-024-09438-6
2. M. Soliman, H. M. Ahmed, N. Badra, T. A. Nofal, I. Samir, Highly dispersive gap solitons for conformable fractional model in optical fibers with dispersive reflectivity solutions using the modified extended direct algebraic method, *AIMS Math.*, **9** (2024), 25205–25222. https://doi.org/10.3934/math.20241229
3. M. Soliman, H. M. Ahmed, N. Badra, I. Samir, Effects of fractional derivative on fiber optical solitons of (2+1) perturbed nonlinear Schrödinger equation using improved modified extended tanh-function method, *Opt. Quantum Electron.*, **56** (2024), 777. https://doi.org/10.1007/s11082-024-06593-3
4. Z. Li, S. Zhao, Bifurcation, chaotic behavior and solitary wave solutions for the Akbota equation, *AIMS Math.*, **9** (2024), 22590–22601. https://doi.org/10.3934/math.20241100
5. R. Hao, L. Li, Z. Li, W. Xue, G. Zhou, A new approach to exact soliton solutions and soliton interaction for the nonlinear Schrödinger equation with variable coefficients, *Opt. Commun.*, **236** (2004), 79–86. https://doi.org/10.1016/j.optcom.2004.03.005
6. W. B. Rabie, H. M. Ahmed, Construction cubic-quartic solitons in optical metamaterials for the perturbed Twin-Core couplers with Kudryashov's sextic power law using extended F-expansion method, *Chaos Solitons Fract.*, **160** (2022), 112289. https://doi.org/10.1016/j.chaos.2022.112289
7. H. U. Rehman, A. F. Aljohani, A. Althobaiti, S. Althobaiti, I. Iqbal, Diving into plasma physics: dynamical behaviour of nonlinear waves in (3+1)-D extended quantum Zakharov–Kuznetsov equation, *Opt. Quantum Electron.*, **56** (2024), 1336. https://doi.org/10.1007/s11082-024-07244-3
8. I. Iqbal, H. U. Rehman, H. Ashraf, A. Walait, N. B. Turki, B. H. Shah, et al., Soliton unveilings in optical fiber transmission: examining soliton structures through the Sasa–Satsuma equation, *Results Phys.*, **60** (2024), 107648. https://doi.org/10.1016/j.rinp.2024.107648
9. M. U. Rahman, S. Ahmad, M. A. Khan, M. Sun, W. F. Alfwzan, A diverse array of optical solitons in the damped (2+1)-dimensional nonlinear Schrödinger equation via the modified exponential rational function method and other distinct strategies, *Opt. Quantum Electron.*, **56** (2024), 959. https://doi.org/10.1007/s11082-024-06705-z
10. M. U. Rahman, M. Sun, S. Boulaaras, D. Baleanu, Bifurcations, chaotic behavior, sensitivity analysis, and various soliton solutions for the extended nonlinear Schrödinger equation, *Bound. Value Probl.*, **2024** (2024), 15. https://doi.org/10.1186/s13661-024-01825-7

11. H. U. Rehman, K. Khushi, I. Iqbal, E. S. M. Sherif, M. U. Shahzad, M. A. Khan, Analysis of optical solitons propagation in the dual-mode resonant nonlinear Schrödinger dynamical equation with assorted nonlinear interactions, *Mod. Phys. Lett. B*, **2024** (2024), 2450433. https://doi.org/10.1142/S0217984924504335

12. I. Iqbal, S. M. Boulaaras, H. U. Rehman, M. S. Saleem, D. Chou, Navigating waves: advancing ocean dynamics through the nonlinear Schrödinger equation, *Nonlinear Eng.*, **13** (2024), 20240025. https://doi.org/10.1515/nleng-2024-0025

13. K. Zhang, J. Cao, J. Lyu, Dynamic behavior and modulation instability for a generalized nonlinear Schrödinger equation with nonlocal nonlinearity, *Phys. Scr.*, **100** (2024), 015262. https://doi.org/10.1088/1402-4896/ad9cfa

14. J. Pan, M. U. Rahman, Rafiullah, Breather-like, singular, periodic, interaction of singular and periodic solitons, and a-periodic solitons of third-order nonlinear Schrödinger equation with an efficient algorithm, *Eur. Phys. J. Plus*, **138** (2023), 912. https://doi.org/10.1140/epjp/s13360-023-04530-z

15. R. C. López, G. H. Sun, O. Camacho-Nieto, C. Yáñez-Márquez, S. H. Dong, Analytical traveling-wave solutions to a generalized Gross–Pitaevskii equation with some new time and space varying nonlinearity coefficients and external fields, *Phys. Lett. A*, **381** (2017), 2978–2985. https://doi.org/10.1016/j.physleta.2017.07.012

16. X. L. Mai, W. Li, S. H. Dong, Exact solutions to the nonlinear Schrödinger equation with time-dependent coefficients, *Adv. High Energy Phys.*, **2021** (2021), 6694980. https://doi.org/10.1155/2021/6694980

17. Z. Wang, K. Zhao, P. Li, Y. Liu, Boundedness of square functions related with fractional Schrödinger semigroups on stratified Lie groups, *Commun. Anal. Mec.*, **15** (2023), 410–435. https://doi.org/10.3934/cam.2023020

18. R. Sun, W. Deng, A generalized time fractional Schrödinger equation with signed potential, *Commun. Anal. Mech.*, **16** (2024), 262–277. https://doi.org/10.3934/cam.2024012

19. M. Kapoor, G. Arora, V. Joshi, Numerical approximation of coupled Schrödinger equations via NUAH B-spline DQM, *Comput. Methods Differ. Equations*, 2025. https://doi.org/10.22034/cmde.2025.64656.2935

20. T. Mayteevarunyoo, B. A. Malomed, Interactions of fractional solitons with local defects: stabilization and scattering, *ArXiv*, 2025. https://doi.org/10.48550/arXiv.2502.17819

21. Y. Zhang, X. Feng, L. Qian, A high-order compact ADI scheme for two-dimensional nonlinear Schrödinger equation with time fractional derivative, *Comput. Appl. Math.*, **44** (2025), 168. https://doi.org/10.1007/s40314-025-03127-9

22. B. Li, Y. Zhang, X. Li, Z. Eskandari, Q. He, Bifurcation analysis and complex dynamics of a Kopel triopoly model, *J. Comput. Appl. Math.*, **426** (2023), 115089. https://doi.org/10.1016/j.cam.2023.115089

23. Z. Eskandari, Z. Avazzadeh, R. K. Ghaziani, B. Li, Dynamics and bifurcations of a discrete-time Lotka–Volterra model using nonstandard finite difference discretization method, *Math. Methods Appl. Sci.*, 2022. https://doi.org/10.1002/mma.8859

24. X. Zhu, P. Xia, Q. He, Z. Ni, L. Ni, Ensemble classifier design based on perturbation binary salp swarm algorithm for classification, *Comput. Model. Eng. Sci.*, **135** (2023), 022985. https://doi.org/10.32604/cmes.2022.022985

25. H. Triki, A. Pan, Q. Zhou, Pure-quartic solitons in presence of weak nonlocality, *Phys. Lett. A*, **459** (2023), 128608. https://doi.org/10.1016/j.physleta.2022.128608

26. M. Vivas-Cortez, G. A. Basendwah, B. Rani, N. Raza, Extraction of new solitary wave solutions in a generalized nonlinear Schrödinger equation comprising weak nonlocality, *PLoS One*, **19** (2024), e0297898. https://doi.org/10.1371/journal.pone.0297898

27. S. Zhao, Z. Li, The analysis of traveling wave solutions and dynamical behavior for the stochastic coupled Maccari's system via Brownian motion, *Ain Shams Eng. J.*, **15** (2024), 103037. https://doi.org/10.1016/j.asej.2024.103037

28. M. Gu, F. Liu, J. Li, C. Peng, Z. Li, Explicit solutions of the generalized Kudryashov's equation with truncated M-fractional derivative, *Sci. Rep.*, **14** (2024), 21714. https://doi.org/10.1038/s41598-024-72610-w

29. Z. Li, J. Lyu, E. Hussain, Bifurcation, chaotic behaviors and solitary wave solutions for the fractional Twin-Core couplers with Kerr law non-linearity, *Sci. Rep.*, **14** (2024), 22616. https://doi.org/10.1038/s41598-024-74044-w

30. S. Zhao, Chaos analysis and traveling wave solutions for fractional (3+1)-dimensional Wazwaz Kaur Boussinesq equation with beta derivative, *Sci. Rep.*, **14** (2024), 23034. https://doi.org/10.1038/s41598-024-74606-y

31. A. Altalbe, A. A. Zaagan, A. Bekir, A. Cevikel, The nonlinear wave dynamics of the space-time fractional van der Waals equation via three analytical methods, *Phys. Fluids*, **36** (2024), 027140. https://doi.org/10.1063/5.0196639

32. M. Gu, J. Li, F. Liu, Z. Li, C. Peng, Propagation of traveling wave solution of the strain wave equation in microcrystalline materials, *Open Phys.*, 2024. https://doi.org/10.1515/phys-2024-0093

33. A. C. Cevikel, A. Bekir, Ö. Guner, Exploration of new solitons solutions for the Fitzhugh–Nagumo-type equations with conformable derivatives, *Int. J. Mod. Phys. B*, **37** (2023), 2350224. https://doi.org/10.1142/S0217979223502247

34. F. Li, J. Wang, Y. Yang, Exact and data-driven lump wave solutions for the (3+1)-dimensional Hirota–Satsuma–Ito-like equation, *Symmetry*, **16** (2024), 1469. https://doi.org/10.3390/sym16111469

35. W. X. Ma, Lump waves and their dynamics of a spatial symmetric generalized KP model, *Rom. Rep. Phys.*, **76** (2024), 108. https://doi.org/10.59277/RomRepPhys.2024.76.108

36. W. X. Ma, Soliton solutions to Sasa–Satsuma-type modified Korteweg–de Vries equations by binary Darboux transformations, *Mathematics*, **12** (2024), 3643. https://doi.org/10.3390/math12233643

37. L. Cheng, Y. Zhang, W. X. Ma, An extended (2+1)-dimensional modified Korteweg–de Vries–Calogero–Bogoyavlenskii–Schiff equation: Lax pair and Darboux transformation, *Commun. Theor. Phys.*, **77** (2024), 035002. https://doi.org/10.1088/1572-9494/ad84d3

38. A. Atangana, E. F. D. Goufo, Extension of matched asymptotic method to fractional boundary layers problems, *Math. Probl. Eng.*, **2014** (2014), 107535. https://doi.org/10.1155/2014/107535

39. Z. Yang, B. Y. C. Hon, An improved modified extended tanh-function method, *Z. Naturforsch. A*, **61** (2006), 103–115. https://doi.org/10.1515/zna-2006-3-401

40. O. El-shamy, R. El-barkoki, H. M. Ahmed, W. Abbas, I. Samir, Exploration of new solitons in optical medium with higher-order dispersive and nonlinear effects via improved modified extended tanh function method, *Alex. Eng. J.*, **68** (2023), 611–618. https://doi.org/10.1016/j.aej.2023.01.053

41. K. K. Ahmed, N. M. Badra, H. M. Ahmed, W. B. Rabie, Soliton solutions of generalized Kundu-Eckhaus equation with an extra-dispersion via improved modified extended tanh-function technique, *Opt. Quantum Electron.*, **55** (2023), 299. https://doi.org/10.1007/s11082-023-04599-x